Flow-induced agitations create a granular fluid

Nichol, K.M.; Zanin, A.; Bastien, R.; Wandersman, E.; Hecke, M.L. van

Flow-Induced Agitations Create a Granular Fluid

Kiri Nichol, Alexey Zanin, Renaud Bastien, Elie Wandersman, and Martin van Hecke
Kamerlingh Onnes Lab, Universiteit Leiden, Postbus 9504, 2300 RA Leiden, The Netherlands
(Received 20 November 2009; published 17 February 2010)

We fluidize a granular medium through localized stirring and probe the mechanical response of quiescent regions far away from the main flow. In these regions the material behaves like a liquid: high-density probes sink, low-density probes float at the depth given by Archimedes' law, and drag forces on moving probes scale linearly with the velocity. The fluidlike character of the material is set by agitations generated in the stirred region, suggesting a nonlocal rheology: the relation between applied stress and observed strain rate in one location depends on the strain rate in another location.

DOI: 10.1103/PhysRevLett.104.078302 PACS numbers: 47.57.Gc, 83.80.Fg

What governs the flow of granular media? At the grain level, interactions are mediated by collisions and contacts [1]. While rapid flows where collisions dominate can be described by advanced kinetic theories [2], and the understanding of flows where both contacts and collisions are important has recently advanced tremendously [3,4], it remains difficult to describe slow flows where enduring contacts dominate the interactions.

Aspects of such slow grain flows can be captured by a frictional rheology in which the friction laws acting at the grain scale are translated to effective friction laws for the stresses acting at a coarse-grained level [5–7]. In such a Mohr-Coulomb picture, granular media remain jammed when the ratio of shear τ to normal stresses P is below a critical value given by an effective friction coefficient, μ, while slowly flowing grains correspond to stresses close to the yielding criterion: $\tau/P \approx \mu$.

This framework is, however, not complete. The combination of rate independence and a sharp yielding criterium leads to a description which predicts the localization of flows in shear bands of vanishing width and a corresponding sharp separation between stationary zones and flowing zones [5]. However, in experiments shear bands are found to be of finite width and the boundary between flowing and stationary zones is not sharp, with creep flow occurring even far away from the main shear band [8–13]. The first key question is therefore: what is the nature of the nearly-stationary zones far away from the main flow? A second key question is motivated by the observation that, for slow flows, the flow rate is independent of the stresses. But if the flow rate is not determined by the stresses what then is the physical mechanism that sets the flow rate of slow granular flows? [3,5,7].

Here we address these questions by locally stirring a container of glass beads at a given rate (Ω) while probing the mechanical response of the essentially quiescent regions near the surface, away from the shear band [Figs. 1(a) and 1(b)]. We find that a heavy object—such as a steel ball—sinks slowly into the sand with a rate proportional to Ω [Fig. 1(a)]. Moreover, low-density objects sink (or rise) to the depth predicted by Archimedes' law [Fig. 1(c)]. Therefore, granular materials do not exhibit a yield stress in the presence of flow: flow fluidizes granular media. By observing the motion of probes immersed in the sand, we find that the drag forces acting on the probes are linear in velocity. This suggests that the material is viscous, although we find that the viscosity depends strongly on filling height, location, and mass of the probes—the rheology of the material is highly nonlinear. Moreover, the relation between applied stress and observed strain rate in one location depends on the strain rate in

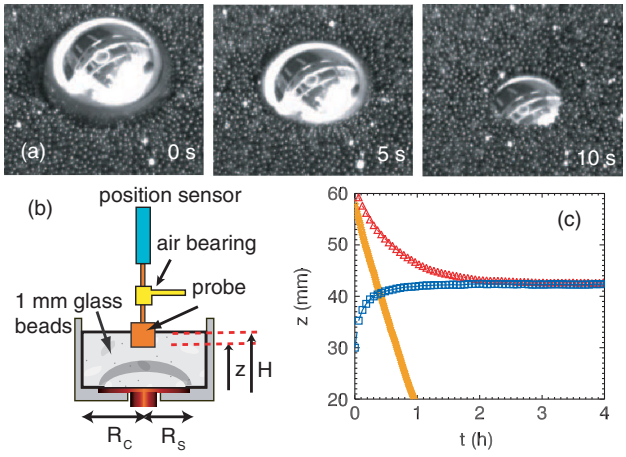

FIG. 1 (color online). (a) Snapshots of a stainless steel ball of diameter 25 mm and mass 64 g, sinking into a stationary granular fluid. The granular fluid is generated in a split-bottom shear cell (inner radius $R_c = 81$ mm, disk radius $R_s = 60$ mm) filled to a height of $H = 60$ mm with millimetric glass beads and driven at a rate $\Omega = 0.1$ rps. (b) Experimental setup, with the domelike shear zone indicated in dark gray. (c) Examples of probe position, z, as function of time, t, for a filling height of $H = 60$ mm. A high-density object sinks in the sand (orange [light gray] $M = 48$ g, $D = 18$ mm, $\Omega = 3 \times 10^{-3}$ rps). A low-density object ($M = 40$ g, $D = 40$ mm, $\Omega = 0.1$ rps) sinks until reaching an equilibrium depth (red [medium gray])—and rises up to this same depth if initially deeply submerged (blue [dark gray]).

another location [14,15]. Our findings highlight novel behavior which we believe to be crucial for the development of better models of slow granular flows [15–17].

Setup.—Our experiment consists of a split-bottom shear cell [6,11,12,16], filled with glass beads of mean diameter $d = 1$ mm to a height H (Fig. 1). The bottom disk (radius $R_S = 60$ mm) is driven by a microstepper motor at a rate, Ω, which ranges from 10^{-4} to 1 rps. The relative humidity of the system is controlled at $8 \pm 2\%$ at room temperature. Prior to beginning a measurement, the grains are stirred with a rod, the grain surface is leveled, and the bottom disk is spun at a rate of 0.5 rps for 20 s. However, we have found no evidence for systematic dependence of the long-time behavior of the probe on the preparation history. Grooves and dimples are machined into the surface of the container and the disk to create a rough boundary and the resulting grain flows have been studied extensively [6,11,12,16].

In order to investigate the liquidlike properties of the system, smooth aluminum cylinders of mass M and diameter D are immersed in the grains. These probes are attached to a shaft that passes through an air bearing, which fixes the horizontal position of the probe while allowing the probe to rotate and to move in the vertical direction. The probe shaft next passes into a linear variable differential transformer (LVDT) position sensor (DC Fastar 2M, accuracy of 2 μm) which we employ to measure the position of the bottom surface of the probe, z.

Phenomenology.—For the large filling heights ($H/R_s > 0.8$) examined here, the shear zone that emanates from the edges of the disk is submerged in the bulk of the material [Fig. 1(b)], and the residual flow observed at the free surface is several orders of magnitude smaller than the driving rate Ω [11,12]. A probe placed at the surface of the beads will get stuck at a small depth if the disk is not rotating (for example, for $D = 30$ mm and $M = 100$ g, the initial depth is less than 5 mm). However, when the disk begins rotating the probe will immediately start to sink into the grains. Heavy probes will continue to sink until they reach the bottom of the container, while light objects reach a well-defined floating depth [Fig. 1(c)]. By observing the motion of such probes we will address the following questions: What sets the floating depth of light objects? Does the material exhibit a yield stress? What governs the drag forces on the probes?

Archimedes' law.—As shown in Fig. 2(a), we have determined the floating depths (z_{eq}) for a series of probes of varying mass. For each mass, three sinking and three rising experiments are conducted—in all cases the equilibrium depths, z_{eq}, are consistent within 0.6 mm. We conclude that there is no appreciable yield stress in the material: if the system did exhibit a yield stress, the sinking and rising probes would reach different equilibrium positions. As shown in Fig. 2(b), the equilibrium depth varies linearly with M. Both this linear dependence and the convergence of the rising and sinking probes to the same floating depth are suggestive of Archimedes' law, which in this case

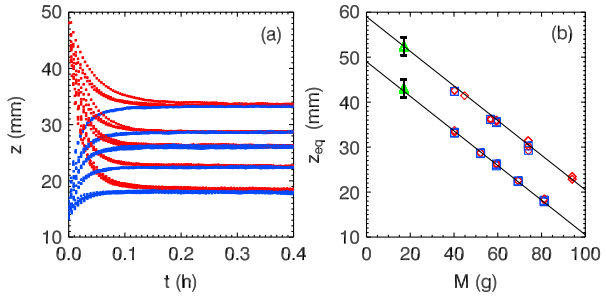

FIG. 2 (color online). (a) Evolution of the probe position (z) for $\Omega = 0.1$ rps, $H = 50$ mm, $D = 40$ mm and five different masses ranging from 40 to 81 g. (b) The equilibrium depths, z_{eq}, as a function of probe mass for $H = 50$, 60 mm and $D = 40$ mm. The red diamonds and blue squares correspond to the sinking and rising cases as shown in panel (a). The green triangles correspond to lighter probes detached from the inductor measurement device and imaged with a CCD camera. The straight lines show Archimedes' law for a density of 1.92 g/cm^3 and finite size correction factor $\kappa = 1.08$—the respective effective heights, $H - \delta H$, are 49 and 59 mm.

reads:

$$z_{eq} = H(z_{eq}) - \delta H - \frac{4M}{\pi(\tilde{D})^2\rho} = H - \delta H - \frac{4M}{\pi D^2 \kappa \rho}. \quad (1)$$

Here, both $\tilde{D}$ and κ are effective parameters that incorporate finite size effects. First, the probe displaces grains as it sinks, so the actual height of the grains, $H(z)$, depends on the probe position. Second, the finite size of the grains suggests that the effective size of the probe, $\tilde{D}$, may be somewhat larger than the real value: $D < \tilde{D} < D + d$. Both effects can be incorporated in the finite size parameter κ—the first effect is of order $1 + (D/(2R_c))^2 \approx 1.06$, the second effect is of order $(\tilde{D}/D)^2$ which ranges from 1 to 1.05—hence we estimate κ to be between 1.06 and 1.11. Finally, we allow for a small correction, δH, which is on the order of a grain size and takes into account the lower packing density of grains near the bottom of the probe. Direct measurement of the mass and volume of well-compacted grains yields a density of 1.92 ± 0.05 g/cm^3.

As shown in Fig. 2(b), the equilibrium depth is well described by Eq. (1) for $\kappa = 1.08$ and $\delta H = d$, where d is the diameter of the beads. The finite size correction, κ, lies within the expected range, and the height correction δH is also small—we thus conclude that Archimedes' law describes the floating depths of our probes accurately, provided that finite size corrections are properly taken into account. Note that Archimedes' law has also been observed in a granular system in which the lateral boundaries are vibrated [18]—but this driving appears far more vigorous than in our system.

Viscous force.—As shown in Fig. 3, the probe position approaches the equilibrium depth exponentially for small $|z - z_{eq}|$ [19]. The data suggest that the characteristic times for rising probes are somewhat smaller than that for sink-

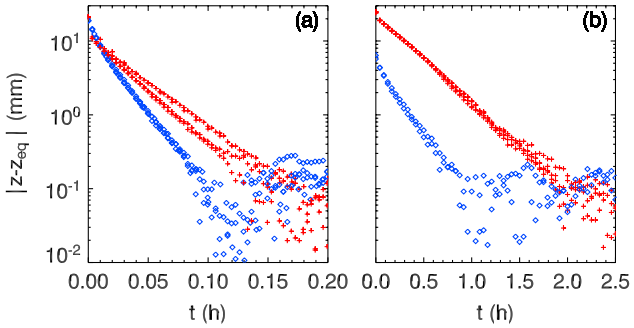

FIG. 3 (color online). Exponential approach to equilibrium depth as demonstrated by sinking probes (red crosses) and rising probes (blue diamonds) for $M = 40$ g, $D = 40$ mm, $\Omega = 0.1$ rps and $H = 50$ mm (a) and $H = 60$ mm (b).

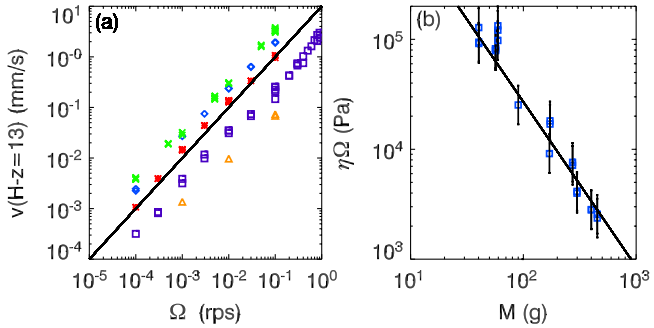

FIG. 4 (color online). (a) Probe velocity 13 mm below the surface as a function of disk rotation speed Ω. Red stars: $H = 60$ mm, $M = 77$ g, $D = 18$ mm. Blue diamonds: $H = 50$ mm, $M = 46$ g, $D = 18$ mm. Purple squares: $H = 60$ mm, $M = 48$ g, $D = 18$ mm. Green crosses: $H = 60$ mm, $M = 86$ g, $D = 18$ mm. Orange triangles: $H = 60$ mm, $M = 46$ g, $D = 18$ mm with a probe immersed at a radius of 15 mm away from the center. The line has slope 1. (b) Rescaled viscosity, $\Omega\eta$, at $z = 50$ mm as a function of probe mass for $D = 40$ mm, $H = 60$ mm. The line is a guide to the eye corresponding to a power law with exponent -1.5.

ing probes, although the apparent slope of the curves is very sensitive to the precise choice of z_{eq}. In the remainder of this Letter we focus primarily on sinking probes where we can vary the probe mass over a wide range.

Since the difference between the gravitational and buoyant forces is linear in z-z_{eq}, the exponential relaxation implies that the drag force (F_d) on a probe is proportional to its velocity. Ignoring geometrical form factors for drag on a cylinder, we define the effective viscosity, η, of the granular fluid using $F_d = -\eta D dz/dt$. Combining this drag force with the buoyant force, F_b, and the gravitational force suggested by Archimedes' law yields the following equation of motion for the probes:

$$\eta D \frac{dz}{dt} = -Mg + F_b. \tag{2}$$

In contrast, previous work [20,21] finds that drag forces on intruders in quiescent or oscillated granular media exhibit a finite threshold.

In the remainder of this Letter we will address the following two questions. (i) How does the effective viscosity depend on the parameters H and M? (ii) Is the viscosity set by the local residual flow near the probe?

Viscosity.—From a wide range of experimental data we conclude that the viscosity is inversely proportional to Ω. In Fig. 4(a) we plot the immersion speed, v, at a fixed depth ($z = H - 13$ mm) as a function of Ω for a number of probes. Clearly, $v \propto \Omega$ over a wide range of disk rotation speeds. The characteristic time scale of the exponential relaxation of floating probes is also proportional to Ω (not shown). Hence, the relevant time scale for probe motion is set by Ω, and internal time scales (such as given by vibrations) appear irrelevant.

In a true liquid, the viscosity is independent of the mass of an object sinking in the system. However, the viscosities of our granular liquids exhibit a surprising dependence on the probe mass [Fig. 4(b)]. Moreover, we found that the precise form of $\eta(M)$ depends strongly on H and weakly on the measurement depth, z. The detailed rheology is complicated and we leave a detailed study to further work.

In Fig. 5(a) we plot the measured viscosity for a single probe ($M = 59$ g, $D = 30$ mm) as a function of z for three values of H (50, 60 and 70 mm). These viscosities are obtained by measuring $z(t)$ and then invoking Eq. (2) to calculate the effective viscosity. From Fig. 5(a) it is apparent that the viscosity depends on the filling height, H. Moreover, the viscosity for a given filling height changes very little with the probe depth, which is consistent with our observation that the trajectory of light probes evolves exponentially over a substantial range. Clearly, the strong dependence on H and the weak dependence on z rules out a picture in which the viscosity simply depends on the distance to the flowing zone.

Nonlocal flow rule.—Even though the flow and strain rates near the free surface are very small, they are not zero [6,11,12]. It is therefore instructive to ask if the probe

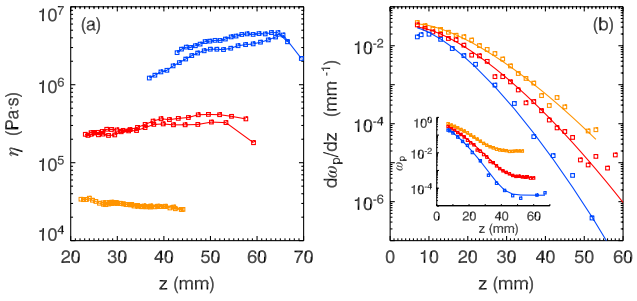

FIG. 5 (color online). (a) Viscosity as a function of probe position for a probe with $M = 59$ g, $D = 30$ mm and $H = 50$, 60 and 70 mm (lower orange curve, middle red curve and upper blue curve, respectively). (b) The variation of the strain rate $\partial_z \omega_p$ with z for $H = 50$, 60 and 70 mm. Inset: ω_p as a function of the height above the spinning disk. Curves are of the form $\omega_p(z) - \omega_p(z = H) \sim \exp(-(z/\xi)^{1.5})$, with $\xi = 9.5$, 11.5 and 13 mm, respectively.

motion is determined by the local residual flow near the probe. To answer this question we will compare the way the viscosity depends on H and z [Fig. 5(a)] to the way the local strain rate varies with H and z. For domelike shear bands, the strain in the region above the center of the disk is torsional [12], and so the strain rate varies as $(\partial_z \omega|_{r=0})$.

We have measured the precession rate, $\omega_p(z) := \omega(z)|_{r=0}/\Omega$, by inserting tiny vanelike probes in the center of the grain flow and observing the rotation of the probe with a rheometer. The resulting precession rates, $\omega_p(z)$, are shown in Fig. 5(b) for $H = 50$, 60 and 70 mm, and are in good qualitative agreement with earlier magnetic resonance imaging (MRI) measurements and simulations [12]. Our larger measurement range allows us to establish that $\omega_p(z)$ approaches the surface precession rate, $\omega_p(z = H)$, faster than an exponential but slower than a Gaussian, and our results are fitted well by an expression of the form $\omega_p(z) - \omega_p(z = H) = \omega_p(z = 0)\exp(-(z/\xi)^{1.5})$, where $\omega_p(z = 0)$ captures slip near the bottom disc, and the characteristic length scale ξ is of order 10 mm.

By either differentiating this expression, or by numerically differentiating the measured data, we can determine $\partial_z \omega_p(z)$: the result is shown in Fig. 5(b). Clearly, the local strain rate and $\eta(z)$ are poorly correlated—while the former changes over four decades for $H = 70$ mm, the latter changes over less than half a decade.

Conclusion and outlook.—By applying localized shear to a container of glass beads we have created a granular fluid with unusual properties. First, our granular fluid does not exhibit the glassy behavior typical of granular media that are agitated by other means such as tapping, vibrations, oscillatory shear or gas-fluidization [22–25]. Moreover, the characteristic time scale is simply set by the inverse driving rate, $1/\Omega$. We speculate that the application of steady shear does not allow for caging and other typical glasslike behavior away from the shear zone, but instead leads to fluidization throughout the material.

Second, the drag forces on the intruder are simply proportional to the velocity. This differs from the behavior observed during the formation of impact craters [26,27] and from earlier observations of slowly dragged intruders [20,21]. Third, our granular fluid does not exhibit a finite yield stress. The disappearance of the yield stress in the presence of distant flow suggests that the stress and strain tensor are colinear, consistent with recent simulations [16], but in strong contrast to the usual Mohr-Coulomb phenomenology [5].

Finally, the local rheology of the material is set by the flow in the stirred region, not by the local residual (creep) flow. We suggest that random grain motion in the flowing zone leads to grain agitations even far away from the flow, and that these agitations generate the liquidlike behavior. Hence, the rheology is nonlocal: the relation between applied stress and observed strain rate in one location depends on the strain rate in another location. Whether this is similar to observations of nonlocal rheology recently observed in emulsions [14] is at present an open question.

We thank J. Mesman for technical assistance and M. Cates for discussions.

[1] H. M. Jaeger, S. R. Nagel, and R. P. Behringer, Rev. Mod. Phys. **68**, 1259 (1996).
[2] I. Goldhirsch, Annu. Rev. Fluid Mech. **35**, 267 (2003).
[3] GDR MiDi, Eur. Phys. J. E **14**, 341 (2004).
[4] P. Jop, Y. Forterre, and O. Pouliquen, Nature (London) **441**, 727 (2006).
[5] R. M. Nedderman, *Statics and Kinematics of Granular Materials* (Cambridge Univ. Press, Cambridge, UK, 1992).
[6] T. Unger *et al.*, Phys. Rev. Lett. **92**, 214301 (2004); J. Török *et al.*, Phys. Rev. E **75**, 011305 (2007); A. Ries, D. E. Wolf, and T. Unger, Phys. Rev. E **76**, 051301 (2007).
[7] R. R. Hartley and R. P. Behringer Nature (London) **421**, 928 (2003).
[8] D. M. Mueth *et al.*, Nature (London) **406**, 385 (2000).
[9] T. S. Komatsu *et al.*, Phys. Rev. Lett. **86**, 1757 (2001).
[10] L. Bocquet *et al.*, Phys. Rev. E **65**, 011307 (2001).
[11] D. Fenistein and D. M. van Hecke, Nature (London) **425**, 256 (2003); D. Fenistein, J. W. van de Meent, and M. van Hecke, Phys. Rev. Lett. **92**, 094301 (2004); D. Fenistein, J. W. van de Meent, and M. van Hecke, Phys. Rev. Lett. **96**, 118001 (2006).
[12] X. Cheng *et al.*, Phys. Rev. Lett. **96**, 038001 (2006).
[13] J. Crassous *et al.*, J. Stat. Mech. (2008) P03009.
[14] J. Goyon *et al.*, Nature (London) **454**, 84 (2008).
[15] L. Bocquet, A. Colin, and A. Ajdari, Phys. Rev. Lett. **103**, 036001 (2009).
[16] M. Depken, W. van Saarloos, and M. van Hecke, Phys. Rev. E **73**, 031302 (2006); M. Depken *et al.*, Europhys. Lett. **78**, 58001 (2007).
[17] R. Gutfraind and O. Pouliquen, Mech. Mater. **24**, 273 (1996).
[18] D. A. Huerta *et al.*, Phys. Rev. E **72**, 031307 (2005).
[19] The noisy behavior seen close to the equilibrium depth is not due to measurement noise but rather to the random motion that the floating probe experiences (of order of 1/10th of a bead diameter or less).
[20] R. Candelier and O Dauchot, Phys. Rev. Lett. **103**, 128001 (2009).
[21] J. F. Geng and R. P. Behringer, Phys. Rev. E **71**, 011302 (2005).
[22] J. B. Knight *et al.*, Phys. Rev. E **51**, 3957 (1995).
[23] P. Umbanhowar and M. van Hecke, Phys. Rev. E **72**, 030301(R) (2005).
[24] O. Dauchot, G. Marty, and G. Biroli, Phys. Rev. Lett. **95**, 265701 (2005).
[25] A. S. Keys *et al.*, Nature Phys. **3**, 260 (2007).
[26] J. R. de Bruyn and A. M. Walsh, Can. J. Phys. **82**, 439 (2004).
[27] H. Katsuragi and D. J. Durian, Nature Phys. **3**, 420 (2007).